

Spectroscopic Study of Titanium Dioxide Thin Films Prepared by Pulsed Laser Deposition

Rahaf Nasri¹, Kamal Kayed^{1*} and Hammoud Al-ourabi¹

¹*Department of physics - Faculty of Science - University of Damascus - Syria.*

Received 11 April 2018, Revised 16 July 2018, Accepted 16 November 2018

ABSTRACT

This paper aims to investigate the effect of different type of target on spectroscopic features of titanium dioxide thin films prepared by laser ablation method. The results of this structural study show that the sample deposited using metallic titanium (Ti) target contains a large proportion of developed rutile phase. However, the sample deposited using pressured annealed disc of titanium oxide (TiO₂) target mainly consists of anatase phase. This study also found that the use of metal targets leads to higher optical transparency and a higher energy band gap.

Keywords: Titanium Dioxide, Thin Film, Laser Ablation, Annealing.

1. INTRODUCTION

Titanium dioxide (TiO₂) is one of the extensively studied transition-metal oxides [9] due to its photo(electro)chemical stability, photoactivity, non-toxicity, and low cost [16]. It has wide applications such as solar cells, gas sensors, air purification [5], water remediation [3], anodes for lithium-ion batteries, self-cleaning glasses [13], cosmetics [15], and antireflection coatings [14].

Titanium dioxide available in three basic crystalline phases and an amorphous phase [4]. The three basic crystalline phases are anatase (tetragonal), rutile (tetragonal), and brookite (orthorhombic). Titanium dioxide thin films are commonly used because of their desirable properties such as chemical stability, good adhesion, high stability against mechanical abrasion and high temperatures [6].

Many deposition methods have been used to prepare titanium films. Physical methods such as Direct Current (DC) or Radio Frequency (RF) magnetron sputtering [7], thermal evaporation [4], and electron beam evaporation [18], Pulsed Laser Deposition (PLD) [17], and chemical methods (such as spin coating sol-gel precursors [15], and Chemical Vapour Deposition (CVD) [1]).

In this paper, the PLD was used as a preparation technique due to its advantages. The ablation of the target preserves its stoichiometry in the thin film [2]. PLD offers many choices of target materials, ambient gas, and pressures enabling the production of different types of films that have various structures [11].

*Corresponding Author: [khmk2000@gmail.com](mailto:khm2000@gmail.com)

2. MATERIALS AND METHODS

Two samples (a and b) of titanium dioxide thin films were deposited on silicon and glass substrates by PLD using Q-switched Nd:YAG pulsed laser from a high-purity target mounted in a vacuum chamber with a background pressure of 1×10^{-4} Pa. The samples were deposited using pure oxygen molecular gas at a pressure of 10 Pa, and the deposition time of 10 minutes. Sample (a) was deposited using a metallic Ti target while sample (b) was deposited using a pressed annealed disc of TiO_2 . The distance between the substrate and the target is 2 cm. The laser beam was focused on the target at an incidence angle of 45° . The deposited films were annealed in air at 400°C .

Infrared (IR) absorption spectra of TiO_2 thin films were carried out using a Bruker Vertex 7 Fourier transform IR spectrophotometer with resolutions of 4cm^{-1} as reference a silicon substrate. The thickness of the films was determined from the cross-section image analyzed using a JEOL-type JSM 6400F Scanning Electron Microscope (SEM). The measured thickness of the sample (a) and sample (b) are 28.1 nm and 57.9 nm, respectively. The surface profile, particle sizes and surface roughness were examined using Nanosurf Easy Scan 2 atomic force microscopy (AFM). The optical transmittance measurements of TiO_2 thin films was performed using a UV-Vis spectrophotometer (CARY 5000) integrated with a sphere (DRA-2500) used to measure the total surface reflectance in the wavelength from 300 nm to 800 nm.

2. RESULTS AND DISCUSSION

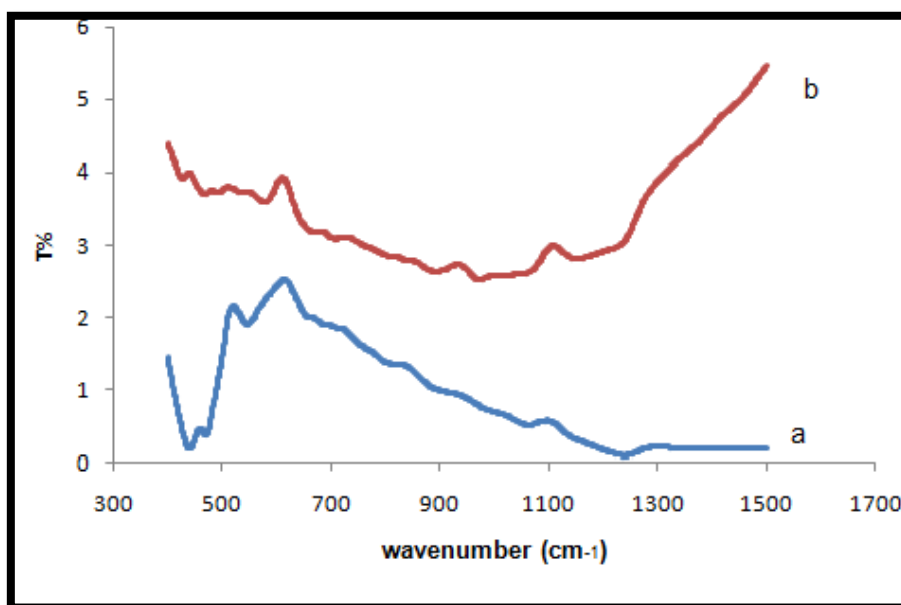


Figure 1. FT-IR spectra for the two samples.

Figure 1 shows the FT-IR transmittance spectra of the two samples. In the case of sample (a), a peak was observed around 445 cm^{-1} , which is the typical characteristic of Ti-O-Ti transverse mode of rutile [8]. The peak at 555 cm^{-1} indicates the presence of titanium metal. In the case of sample (b), two peaks were observed at 431 cm^{-1} and 582 cm^{-1} which are assigned to the stretching mode of anatase [10]. A set of peaks appeared in both spectra: the peaks observed at 1075 cm^{-1} is assigned to C-O stretching mode, where the peaks observed at 667 cm^{-1} and 1246 cm^{-1} are assigned to C=O stretching mode. The peak appears around 475 cm^{-1} probably originated from the presence of Ti-O-Ti bonds [8,10].

Table 1 The elemental compositions analysed using Energy-dispersive X-ray Spectroscopy

Sample a			Sample b		
Element	Weight %	Atomic %	Element	Weight %	Atomic %
C K	5.31	8.37	C K	7.48	11.76
O K	68.9	81.45	O K	65.94	77.77
Ti K	25.79	10.18	Ti K	26.58	10.47

The elemental compositions analysed with Energy-dispersive X-ray Spectroscopy (EDS or EDX) are shown in Table 1. There is a similarity denoted in the components of the films but the percentage of oxygen is slightly lower in sample (b). Carbon is the result of adsorption on the surface of the films.

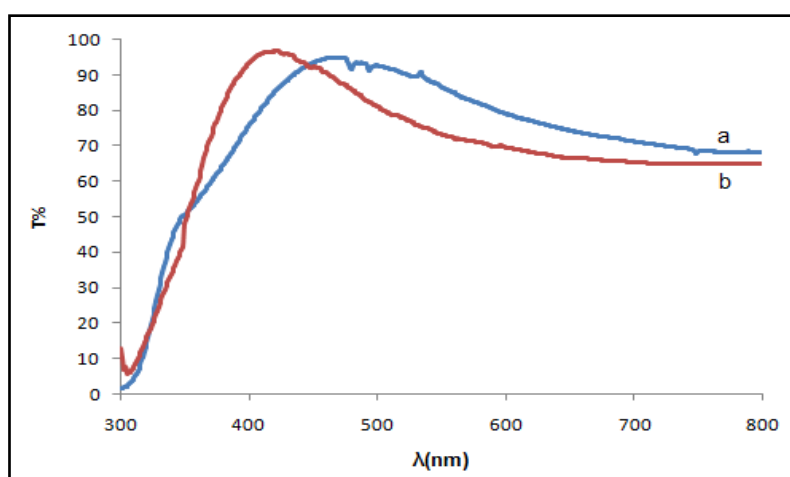


Figure 2. The optical transmissions for the prepared samples.

The transmittance spectra of the TiO_2 prepared films in the wavelengths range of 300–800 nm are shown in Figure 2. Sample (a) has higher optical transparency compared to sample (b). The transmittance difference is the result of several factors where the significant factors are different thickness, density, and crystalline structure. On the other hand, it can be seen that the transmittance spectra show a resonant increase in transmittance at a wavelength of 458 nm for the sample (a) and 410 nm for the sample (b). The increase in transmittance is due to the localized surface plasmon and scattering of photons caused by the photon-electron interaction that decreases the transmittance at longer wavelengths [7]. The peak position shift from 410 nm (sample b) to 458 nm (sample a) indicating that sample (a) has a larger Plasmon particle size compared to sample (b). On the other hand, Figure 2 shows that the plasmon absorption band of sample (a) is larger than sample (b) which means that sample (b) has a higher density of plasmon particles. These results are consistent with the results of EDX measurements (refer to Table 1) where sample (b) has the least oxygen content and higher titanium metal content. These conditions allow a higher proportion of free titanium atoms to form plasmon. Free metal atoms were formed from the disintegration of the TiO_2 oxide when exposed to the laser beam.

Regardless of the effects of plasmon formation, there is no significant difference in the optical transmissions between the two samples. By taking into account the thickness of the two samples, it can be concluded that sample (a) should have high density compared to the sample (b) in order to obtain equal values of the optical transmissions.

The curves in Figure 3 are used to calculate the absorption coefficient and the optical energy gap. The optical gap was calculated for all samples using the relation [12]:

$$\alpha h\nu = A(h\nu - E_g)^{1/2} \quad (1)$$

Where E_g is the optical band gap and A is a constant. The value of E_g can be found by plotting the variation of $(\alpha h\nu)^2$ against $h\nu$, where the extrapolation of the linear region of the curve with x-axis gives the value of the optical band gap of a thin film. Figure 3 below shows the method of calculating the energy band gap of samples.

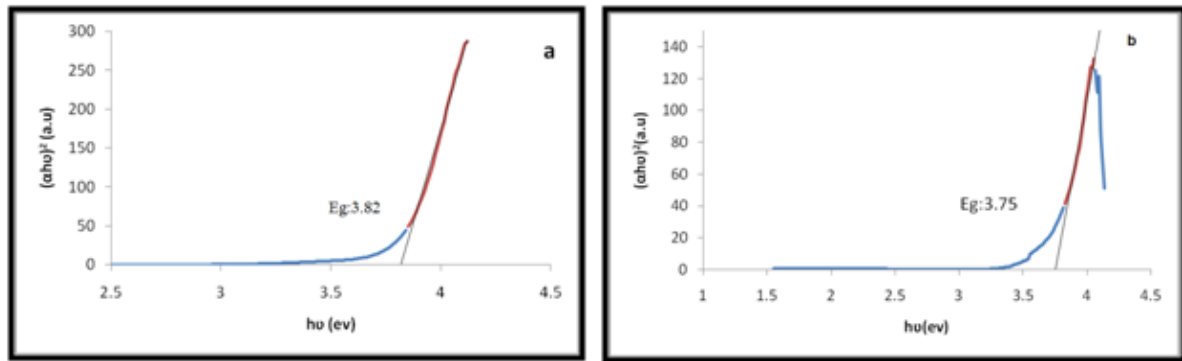


Figure 3. Variation of $(\alpha h\nu)^2$ against $h\nu$ for samples.

The band gap of the sample (a) was 3.82 eV, and the band gap of the sample (b) was 3.75 eV. The decrease in the band gap of the sample (b) compared to sample (a) is consistent with the EDX measurements (Table 1) where sample (b) has a high concentration of plasmon compared to sample (a). Another possible reason is the changes in the crystalline structure and the formation of the anatase phase.

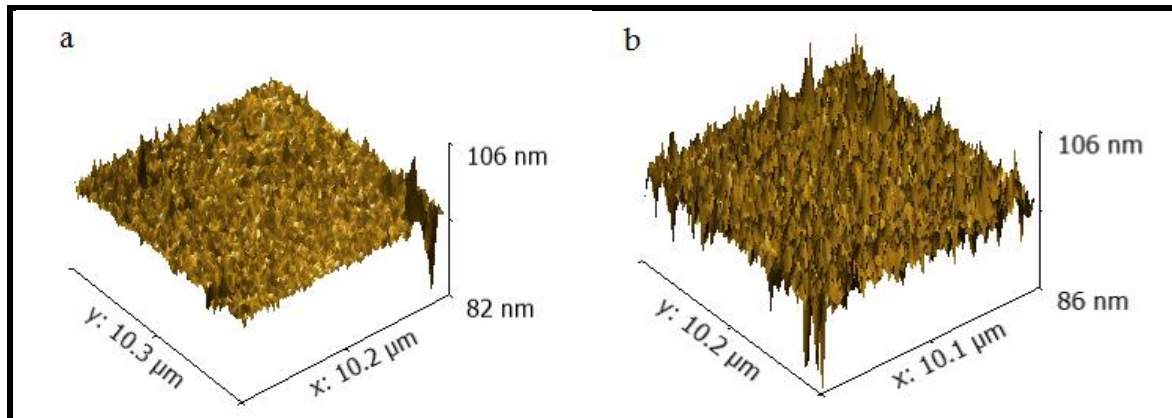


Figure 4. AFM images for the two samples.

The three-dimensional AFM images of the prepared films were presented in Figure 4. The microstructures of the thin films changed depending on the target type. The films have a continuous nanoscale structure with no well-defined grain boundaries. On another hand, sample (b) contains more grain and semi-larger diameters compared to the grain in the sample (a). The roughness of sample (a) is 0.60 nm while the roughness of sample (b) is 0.85.

4. CONCLUSION

TiO₂ thin films were successfully synthesized on silicon and glass substrates using PLD techniques with subsequent annealing in air. The structural and optical properties of TiO₂ thin films were investigated using FTIR and UV-Vis spectroscopes. Results showed that the crystal structure of the film is largely related to the type of target used during the preparation process. In the case when Ti was used as a target, a lower concentration of surface Plasmon was obtained. Whereas, when TiO₂ was used as a target, a higher surface Plasmon concentration with smaller plasmon particle size was obtained. This study also found that the use of metal targets leads to higher optical transparency and lower energy band gap.

ACKNOWLEDGEMENTS

The author would like to thank Dr A. Alkhawwam (A E C S), Dr M. El-Daher and Mr M. Odeh (Department of Physics - Faculty of Science - University of Damascus) for their assistance.

REFERENCES

- [1] Ahn, K. H., Park, Y. B., Park, D. W., Surface and Coatings Technology. Commun. 171.1-3 (2003) 198-204.
- [2] Al-Obaidi, S. S., Yousif, Y., J. Ibn Al-Haitham, Journal for Pure and Applied Science .Commun. 26.3 (2017) 143-152.
- [3] Balasubramanian, G., Dionysiou, D. D., Suidan, M. T., Baudin, I., Lainé, J. M., J. Applied Catalysis B: Environmental. Commun. 47.2 (2004) 73-84.
- [4] Bedikyan, L., Zakhariyev, S., Zakhariyeva, M., Journal of Chemical Technology and Metallurgy. Commun 48.6 (2013) 555-558.
- [5] Boonen, E., Beeldens, A., J. Coatings. Commun 4 (2014) 553-573.
- [6] Dakka, A., Lafait, J., Abd-Lefdil, M., Sella, C., J.MJ Condensed matter. Commun 2.1 (1999) 153-156.
- [7.] El-Raheem, M. A., Al-Baradi, A. M., Journal of Physical Sciences. Commun 8.31 (2013) 1570-1580.
- [8] Ivanova, T., Harizanova, A., Koutzarova, T., Vertruyen, B., Journal of Physics: Conference Series. IOP Publishing. 764.1 (2016) 012019.
- [9] Karunagaran, B., Kim, K., Mangalaraj, D., Yi, J., J. Solar energy materials and solar cells. Commun 88.2 (2005) 199-208.
- [10] Khalid, N. R., Ahmed, E., Rasheed, A., Ahmad, M., Ramzan, M., Shakoore, A., Niaz, N. A., J. Ovonic Res. Commun 11 (2015) 107-112.
- [11] Nakamura, T., Matsubara, E., Sato, N., Muramatsu, A., Takahashi, H., J. Materials Transactions. Commun. 45.7 (2004) 2068-2072.
- [12] N. Mott, E. Davis, Electronic properties in non-crystalline materials, first ed., Oxford University, (1971).
- [13] Promnopas, W., Promnopas, S., Phonkhokkong, T., Thongtem, T., Boonyawan, D., Yu, L., Thongtem, S., J. Surface and Coatings Technology. Commun 306 (2016) 69-74.
- [14] Said, N. M., Sahdan, M. Z., Senain, I., Bakri, A. S., Abdullah, S. A., Mokhter, F., Saim, H., J. ARPN Journal of Engineering and Applied Sciences. 11 (2006) 4924-4928.
- [15] Vetrivel, V., Rajendran, K., Kalaiselvi, V., J. ChemTech Res. Commun 7 (2015) 1090-1097.
- [16] Wu, Z., Xue, Y., Zou, Z., Wang, X., Gao, F., J. Journal of colloid and interface science. Commun 490 (2017) 420-429.
- [17] Xu, Y., Shen, M., Journal of materials processing technology. Commun. 202 (2008) 301-306.

- [18] Xu, Z. J., Zhang, F., Zhang, R. J., Yu, X., Zhang, D. X., Wang, Z. Y., Chen, L. Y., J. Applied Physics A. Commun. 113.3 (2013) 557-562.
- [19] Yang, H., Zhu, S., Pan, N., Journal of Applied Polymer Science. Commun 92.5 (2004) 3201-3210.